ELECTROMAGNETIC RADIATION OF NEURITES

Bogdan-Mihai GAVRILOAIA[1], Mariuca-Roxana GAVRILOAIA[2], Nicolae MILITARU[3], Teodor PETRESCU[4], Nicolae-Dragos VIZIREANU[5]

Neuron, the anatomical unit of the nervous system, processes the information received as coded pulses and generates stereotype pulses sent to other neurons through axon buttons. Current technology does not allow in vivo evaluation of the electrical activity of a single neuron and electromagnetic field detected on scalp is determined by the activity of a set of neurons acting only at macro scale level. The authors present an original method for the analysis of electromagnetic radiation of a network composed of microstrip lines modelling biological neuron by using a proper space transformation. The electrical component distribution and the radiation patterns are evaluated for different resonance frequencies of a given simulated neuron. It demonstrates the capability of the network of antennas, with segments of lines automatically switched depending on the frequency of the emitted signal, for wireless transmission data to other neurons, spatially distributed.

Keywords: Biological Neuron, Electromagnetic Field, Radiation Pattern, Evoked Potential, Neurites

1. Introduction

The perception of the environment is an important feature of living beings and is the result of a long process of historical evolution of biological systems, integrated structures, robust, sophisticated and adaptable. The brain, the most complex biological structure of the universe, integrates data taken from environment by specific sensors and generates impulses that informs or acts on different parts of the human body [1].

Structure and dynamics of the elements of the nervous system are matters not fully elucidated in the field of neuroscience [2, 3]. Important causes of these limitations are given by very large dynamic range of scales at which events occur,

[1] PhD Student, Telecommunications Dpt., University POLITEHNICA of Bucharest, Romania, e-mail: bogdan.gavriloaia@gmail.com
[2] PhD, "Carol Davila" University of Medicine and Pharmacy, Bucharest, Romania, e-mail: roxana.gavriloaia@gmail.com
[3] Associate Prof., Telecommunications Dpt., University POLITEHNICA of Bucharest, Romania, e-mail: nicolae.militaru@munde.pub.ro
[4] Prof., Telecommunications Dpt., University POLITEHNICA of Bucharest, Romania, e-mail: teodor.petrescu@munde.pub.ro
[5] Prof., Telecommunications Dpt., University POLITEHNICA of Bucharest, Romania, e-mail: dragos.vizireanu@upb.ro

their physical support and technological level which must allow access of knowledge [4, 5]. Thus, the fluctuations of different kind of ions take place at nanoscale level, at microscale level is the physical support of neurons, the mesoscale level are the cortical columns, and at macroscale is investigated phenomena from cortical areas with areas of extra-inches square. According to the current technology, in vivo observation of phenomena is done at the macroscale level. For instance, the fMRI image processing can provide a spatial resolution by voxel at about 1 mm^3. In such volume of cortex there are approximately 10^6 neurons connecting to other neurons by 10^{10} synapses.

At the same time, the minimum period for the acquisition of a data set is of the order of seconds, but more than 1000 pulses can pass through one neuron in that interval. A good temporal resolution can be obtained by encephalography investigations, but spatial resolution is much lower. Therefore, in vivo practical knowledge of the biological activity of a single neuron is limited.

In vitro experiments have been successful in obtaining data on the morphology of several types of neurons and developing, on the basis, of new theories regarding the dynamic processes that would enrich the knowledge of science and explaining some of the many experimentally observed phenomena.

One of these important phenomena is the evoked potential. This refers to the electrical activity of neurons that can be measured outside the head, on the scalp, by measuring the intensity of electromagnetic field using wet electrodes type Ag/AgCl or dry [6, 7, 8]. Analysis of the activity on the specific areas of the brain to the application of the auditory, visual or sensorial stimuli provides to neurologists physicians important medical information regarding the health status or certain dysfunctions of anatomical structures concerned.

Starting from the idea that evoked potential is the result of the electric actions carried out at neuron level, this paper investigates the radiation patterns of a biological neuron whose geometric parameters are processed from an international database. The physical support is a network of microstrip lines, and the field radiation is analyzed considering the resonant excitation by harmonic signals. It demonstrates the capability of the network of antennas, with segments of lines automatically switched depending on the frequency of the emitted signal, for wireless transmission data to other neurons, spatially distributed.

2. Material and Methods

Electrical phenomena occurring in the cortical unmyelinated neurons are carried out at speeds between 0.1 m/s and 1 m/s, in intervals of milliseconds and on distances of tens of microns. They can be studied through the similarity with those that occur with the speed of light, if the unit of time is picosecond and the distances grow of thousand times [9]. In this case, the methods and techniques

specific to microwave engineering can be used [10, 11]. The sophisticated geometric configuration of microstrip structures modelling the neuron requires Maxwell's equations for investigation of the electromagnetic field propagation. The six components of the electromagnetic field are solutions of the following matrix equation:

$$\begin{bmatrix} \nabla \mathrm{x} & j\omega\mu \\ -j\omega\varepsilon & \nabla \mathrm{x} \end{bmatrix} \begin{bmatrix} \vec{E} \\ \vec{H} \end{bmatrix} = \begin{bmatrix} 0 \\ \vec{J}_c \end{bmatrix} \tag{1}$$

where $\vec{E}$, $\vec{H}$, and $\vec{J}_c$ are the electric field, magnetic field intensities, and conductive current density, respectively, all of them are harmonic functions. ε and μ are the parameters of the environment where the field propagation takes place [12]. The most widely used methods of problem-solving (1) are the numerical methods assuming the spatial mesh [13].

The field in which the analysis is done has to be decomposed into elements of parallelepiped volume (identified by Yee cell {i, j, k} [14]), where the components of the field are considered to be constants. From (1), the following equations are obtained:

$$\frac{E_z^{i,j+1,k} - E_z^{i,j,k}}{\Delta_y^j} - \frac{E_y^{i,j+1,k} - E_y^{i,j,k}}{\Delta_z^k} = -j\omega\mu_x^{i,j,k} H_x^{i,j,k} \tag{2.1}$$

$$\frac{E_x^{i,j,k+1} - E_x^{i,j,k}}{\Delta_z^k} - \frac{E_x^{i+1,j,k} - E_x^{i,j,k}}{\Delta_x^i} = -j\omega\mu_y^{i,j,k} H_y^{i,j,k} \tag{2.2}$$

$$\frac{E_y^{i+1,j,k} - E_y^{i,j,k}}{\Delta_x^i} - \frac{E_x^{i,j+1,k} - E_x^{i,j,k}}{\Delta_y^j} = -j\omega\mu_z^{i,j,k} H_z^{i,j,k} \tag{2.3}$$

$$\frac{H_z^{i,j,k} - H_z^{i,j-1,k}}{\tilde{\Delta}_y^j} - \frac{H_y^{i,j,k} - H_y^{i,j-1,k}}{\tilde{\Delta}_z^k} = j\omega\varepsilon_x^{i,j,k} E_x^{i,j,k} + J_x^{i,j,k} \tag{2.4}$$

$$\frac{H_x^{i,j,k} - H_x^{i,j,k-1}}{\tilde{\Delta}_z^k} - \frac{H_z^{i,j,k} - H_z^{i-1,j,k}}{\tilde{\Delta}_x^i} = j\omega\varepsilon_y^{i,j,k} E_y^{i,j,k} + J_y^{i,j,k} \tag{2.5}$$

$$\frac{H_y^{i,j,k} - H_y^{i-1,j,k}}{\tilde{\Delta}_x^i} - \frac{H_z^{i,j,k} - H_z^{i,j-1,k}}{\tilde{\Delta}_y^j} = j\omega\varepsilon_z^{i,j,k} E_z^{i,j,k} + J_z^{i,j,k} \tag{2.6}$$

where $\tilde{\Delta}_m^n = \frac{\left(\tilde{\Delta}_m^{n-1} + \tilde{\Delta}_m^{n+1}\right)}{2}$. The present set of relationships is applicable for all N elements of the volume of the meshed ($N = N_x \cdot N_y \cdot N_z$) where N_t is the number of elements in the direction of *t*. Finally we obtain the general form equation:

$$\mathbf{Ax} = \mathbf{b} \tag{3}$$

where **x** and **b** are column vectors of the electromagnetic field components, respectively, and **A** is an spatial operator formed by the coefficients of vectors $\vec{E}$ and $\vec{H}$, containing data related to the geometry of the domain in which the radiated field is analyzed. Equation (3) determines the resonance frequencies of the model, and distributions of electromagnetic field components.

The physical system modeled was the P44 DEV 192 biological neuron of a rat, and its morphometric parameters were taken from the database NeuroMorpho.org [15], NeuroMorpho.Org ID: NMO_04148.

The dendritic tree topology is illustrated in Fig. 1. (a). In Fig. 1 (b) is shown the model realized by using the microstrip lines of 2 mm as width on FR4 dielectric type support. All dimensions shown in this paper are in mm.

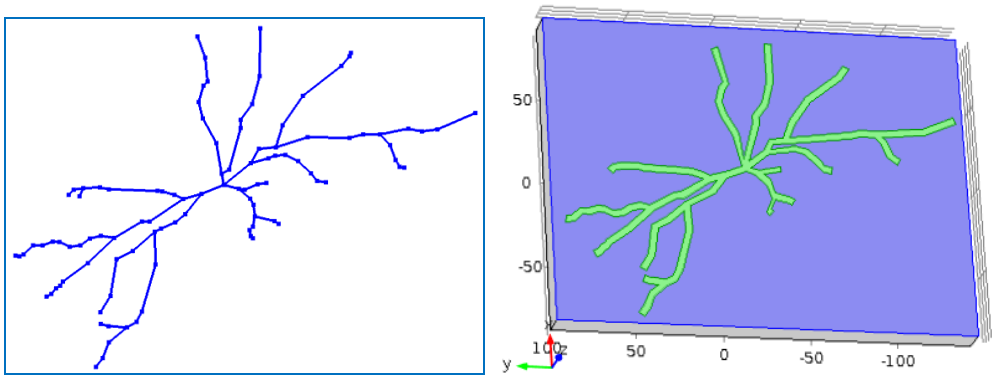

(a) (b)

Fig. 1. The dendritic tree of P44 DEV- 192 (a) and the modeled microstrip network (b)

3. Results and Discussions

The microstrip line network modelling the biologic neuron is enclosed into a sphere with the outer surface built from a 20 mm perfectly matched layer (PML). The layout used for microwave analyses is shown in Fig. 2. By applying the Maxwell equations on the inner environment, a particular form of (3) is obtained. The first 30 eigenvalues of (3) corresponding to the own resonant frequencies of the microstrip line network are presented in Table 1.

The frequency dependence versus harmonic number is shown in Fig. 3 (a). In the same graphic is presented the dependence of the resonant frequencies of the

half wave resonator, as reference. Because the network has many microstrip lines with different lengths, there is no linear dependence between the values of the resonant frequencies and the number of the spatial harmonics, as in the case of the half wave resonator. Also, the curve is not as smooth, and its slope is lower.

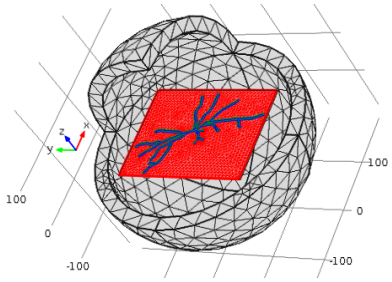

Fig. 2. The layout of the microstrip lines in a spherical enclosure with perfectly matched layer

Table 1

The resonant frequencies of the microstrip line network

Nr. harmonic	Frequency [GHz]	Nr. harmonic	Frequency [GHz]	Nr. harmonic	Frequency [GHz]
1	0.2503	11	0.9058	21	1.7652
2	0.3538	12	1.0681	22	1.7938
3	0.3748	13	1.1619	232	1.8137
4	0.5255	14	1.2995	24	1.9179
5	0.5540	15	1.3337	25	1.9418
6	0.5770	16	1.3820	26	2.1444
7	0.6700	17	1.4151	27	2.1564
8	0.7293	18	1.4904	28	2.1894
9	0.8545	19	1.6342	29	2.2329
10	0.8817	20	1.6524	30	2.3160

The spectrum distribution of amplitudes normed at maximum value of each spectral component is shown in Fig. 3 (b). This amplitude distribution versus frequency is specific to each geometric configuration, or, in other words, to the morphometry of each biological neuron. Such configuration of microstrip lines acts as compact multiple pass-band filter, which are well suited for applications in wireless communications, including as antenna array. The main problem is the electromagnetic field distribution along microstrip lines, because it strongly depends on the operating frequency. The electric field distribution along the microstrip lines is shown in Fig. 4 (a). It is very important to notice that there are some microstrip line where the electric field amplitude is zero. This means these lines cannot be excited by electromagnetic field and, in the same time, they do not contribute to radiation pattern. The entire electric field distribution of the field is somewhat similar that of a dipole distribution.

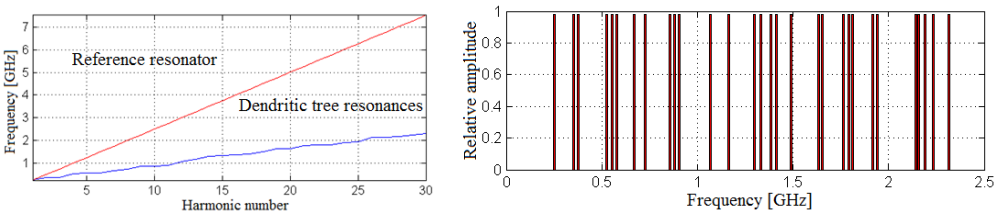

(a) (b)

Fig. 3 Comparative analysis of resonant frequencies between reference and dendritic tree resonator (a) and spectral distribution (b)

The spatial radiation pattern is shown in Fig. 4 (b). There are two directions where the amplitude has higher values. The rectangular coordinates representation, as in Fig, 5, allows to evaluate parameters like gain or directivity. For instance, the maximum gain is 4.37 dBd (from the blue curve).

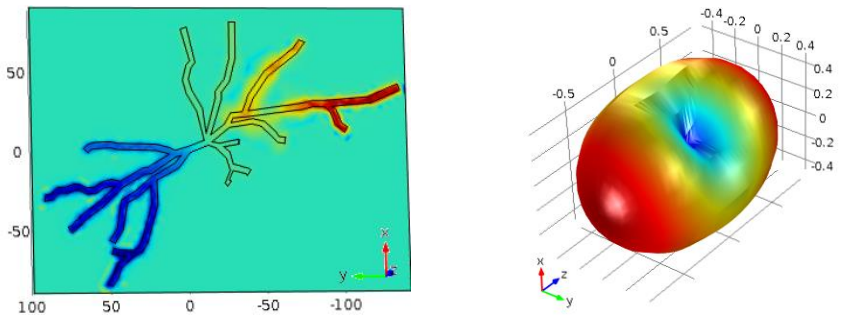

(a) (b)

Fig. 4 Electric field distribution on the microstrip lines for the first resonant frequency (a) and the spatial radiation pattern (b)

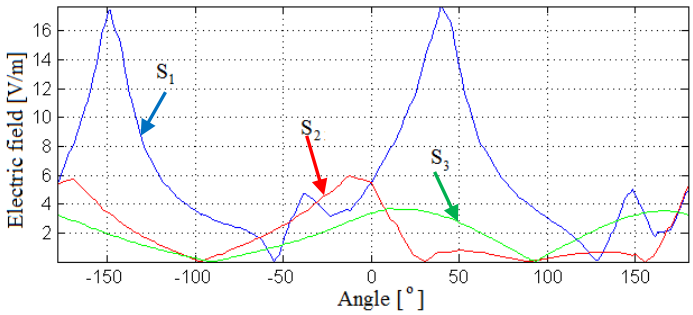

Fig. 5 Rectangular radiation patterns into three orthogonal planes

The original representation, and very easy to understand is illustrated in Fig. 6. It presents the distribution of the electric field on the surfaces of two

hemispheres between which the network of microstrip lines is located. It can be immediately seen where and how the microstrip model radiates when a signal with the first resonant frequency is applied.

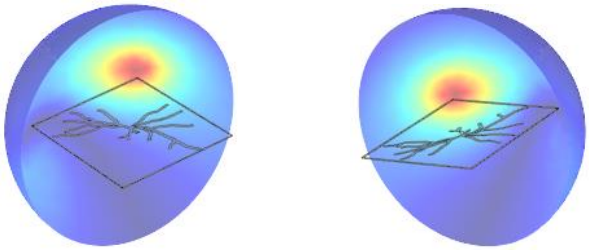

(a) (b)

Fig. 6 Radiation patterns on the left (a) and right hemispheres at the first resonant frequency

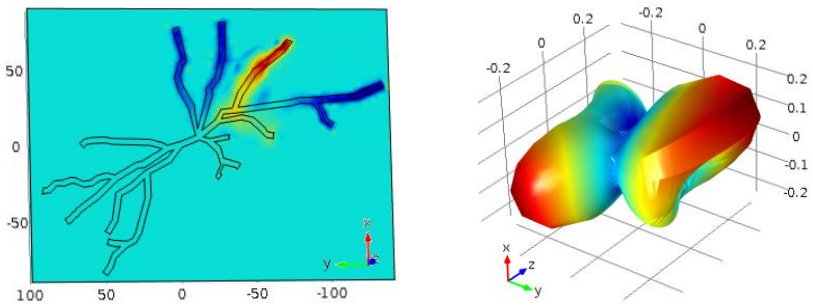

(a) (b)

Fig. 7 Electric field distribution for the fourth resonant frequency (a) and the spatial radiation pattern (b)

The field distribution along microstrip lines and spatial radiation patterns are completely changed when the fourth resonant frequency is applied, as in Fig. 7. The images from Fig. 8 (a) and (b) offer more details than Fig. 7 (b).

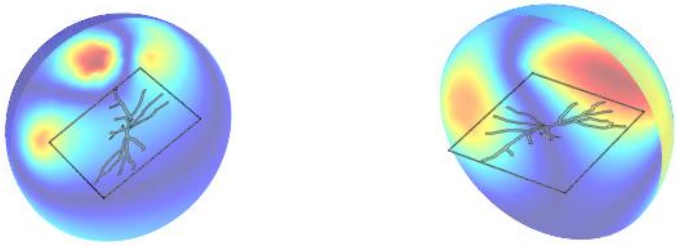

(a) (b)

Fig. 8 Radiation patterns on the left (a) and right (b) hemispheres at the fourth resonant frequency

4. Conclusions

A network with interconnected microstrip lines was used to model a biological neuron. The resonant characteristics and radiation patterns were simulated by using specific methods from microwave engineering in order to prove, for the first time, the resonant behavior of the neural dendritic network, theoretically proposed in the literature for one branch only, and the evoked potential measured on the scalp. The theoretical results can be used for studying the resonance of some interconnected neurons forming cortical columns or having a synchronized oscillatory activity.

R E F E R E N C E S

[1]. *M. Bart, R. Har*, Front-End Vision and Multi-Scale Image Analysis- Multi-Scale Computer Vision Theory and Applications, written in Mathematics - Springer International Publishing AG. Part of Springer Nature, 2017.
[2]. *G. Marcus, J. Freman, M.-Britt, E. Moser*, The Future of the Brain: Essays by the World's Leading Neuroscientists, Princeton University Press, 2014.
[3]. *D. Redish, J. A. Gordon*, Computational Psychiatry , New Perspectives on Mental Illness, The MIT Press, 2016
[4]. *O. Sporns*, Netwrks of the Brain, The MIT Press, 2010
[5]. *M. S. Gazzaniga, R. B. Ivry, and G. R. Mangun*, Cognitive Neuroscience - The Biology of the Mind, W. W. Norton & Company, 2008
[6]. *P.Velazquez, G. Dominguez, G. Erra R*, Fluctuations in neuronal synchronization in brain activity correlate with the subjective experience of visual recognition. J Biol Phys 33:49–59. (2007a)
[7]. *J. R. Glausier | D. A. Lewis*, Dendritic spine pathology in schizophrenia, Neuroscience, Volume 251, 22 October 2013, Pages 90-107
[8]. *Qi, Zhao*, Computational and Cognitive Neuroscience of Vision, Springer Singapore, 2017
[9]. *B-M. Gavriloaia, M. Novac, D-N. Vizireanu*, Microwave Microstrip Antenna Bio-inspired from Dendritic Tee, 3rd EAI International Conference on Future Access Enablers of Ubiquitous and Intelligent Infrastructures, October, 2017, Bucharest, Romania (in press)
[10]**.** *B. Gavriloaia, D. Vizireanu , M. Novac, C. Mara*, Time Domain Analysis of Microstrip Line Network Simulating a Natural Neuron, Proc. of Electronics, Computers and Artificial Intelligence, Targoviste, Romania, 2017.
[11]. *T. Lindeberg*, Time-causal and time-recursive spatio-temporal receptive fields, Journal of Mathematical Imaging and Vision, pp. 50-88, 2016.
[12]. *D. Davidson*, Computational Electromagnetics for RF and Microwave Engineering, 2nd Edition, Cambridge University Press, 2010.
[13]. *P. Sumithra1, D. Thiripurasundari*, A review on Computational Electromagnetics Methods, Advanced Electromagnetics, Vol. 6, , pp. 42-45, 2017.
[14]. *J. Mao, L. Jiang, L. Luo*, A novel space-stepping finite-diference frequency-domain method for full wave electromagnetic field modeling of passive microwave devices. Appl. Comput. Electrom. 24, pp. 259-267. 2009
[15]. http://neuromorpho.org/neuron_info.jsp?neuron_name=P44-DEV192